



COMPUTATION OF ELECTRON IMPACT TOTAL IONIZATION CROSS SECTIONS FOR Ba, Pb and U ATOMS

Avani Barot* and Minaxi Vinodkumar

V. P. & R. P. T. P. Science College, Vallabh Vidyanagar-388 120, Gujarat, India

ABSTRACT

In this paper we report calculations of the total ionization cross sections, Q_{ion} , for atoms, namely Ba, Pb and U, upon electron impact for energies from circa threshold to 2000 eV. Spherical complex optical potential (SCOP) formalism is employed to evaluate total inelastic cross sections, Q_{inel} . Total ionization cross sections, Q_{ion} , are extracted from the total inelastic cross sections, using a semi-empirical formalism developed by us, called the 'complex spherical potential-ionization contribution' (CSP-ic) method. The present results are compared with both theoretical and experimental data available in the literature and overall good agreement is observed for all the reported atoms.

Keywords: Spherical complex optical potential, Complex spherical potential-ionization contribution.

INTRODUCTION

Electron collisions with atoms/ molecules are characterized by two important phenomenon viz. elastic scattering and inelastic scattering which are quantitatively accounted by total elastic cross sections and total inelastic cross sections. The present work deals with total ionization cross sections and hence we will restrict our discussion to the inelastic channel only. The inelastic cross sections are the result of two vital processes viz. electronic excitations and ionization. Electron impact ionization is the most fundamental process and has wide spread applications. It is employed to understand the dynamics of the collision process, structure of the target, to sustain gas discharge, in the chemistry of radiation effects, is the basis for mass spectrometry. Owing to practical importance in diverse fields such as astrophysics, radiochemistry, mass spectrometry etc. electron impact total cross sections are measured since the earliest days of atomic collision physics [1-2].

In the present work we report electron impact total ionization cross sections for three atoms Ba, Pb and U that are very important looking into their applications. Out of the three atoms studied here, Barium has lowest atomic number ($Z = 56$). There are two measurements of total ionization cross sections available by Dettmann and Karstensen [3] and Vainshtein et al [6] and computations of total ionization cross section available by three groups viz. McGuire [4], Vainshtein et al [6] and Talukder et al [5].

Lead is a soft, malleable metal which is included in the group of heavy metals. Lead ($Z = 82$) has the highest atomic number of all of the stable elements and it finds its application in building construction, lead-acid batteries, bullets and shots, weights, as part of solders, pewters, fusible alloys and as a radiation shield. Electron impact total ionization cross sections for lead is measured by two groups, Freund et al [9] and McCartney et al using pulsed crossed-beam technique [10] and calculated by Kim and Stone [11] and Talukder et al [5] employing empirical formula. There is very large discrepancy 54% between the two measurements at 100 eV.

Uranium ($Z = 92$) is a hard, dense, malleable, ductile, silver-white, radioactive toxic metal. It gained its importance due to its use in nuclear energy and manufacture of atom bombs. Measurements of electron

impact total ionization cross sections is difficult [12] and hence reported by only two groups Halle et al [13] and Blackburn and Danielson [14]. Halle et al [13] measured electron impact single and multiple ionization cross sections for uranium for impact energies 6.5 eV to 500 eV using modulated crossed-beam method. Blackburn and Danielson [14] measured electron impact total ionization cross section for uranium over the same energy range (6.5 eV to 500 eV). There is very large discrepancy [55%] between the two measurements at 25 eV [13, 14]. Theoretically electron impact total ionization cross sections are predicted by [5, 15-17].

THEORETICAL METHODOLOGY

The electron atom/molecule scattering phenomenon is characterized quantitatively by two important cross sections viz. total elastic and total inelastic cross sections and they combine to represent total cross sections. Accordingly we have,

$$Q_T(E_i) = Q_{el}(E_i) + Q_{inel}(E_i) \quad (1)$$

where the first term on the right hand side accounts for all elastic processes while the second term takes care of loss of flux in the outgoing channel resulting from electronic excitations and ionization. We are interested here in the total ionization cross sections and hence the second term of equation (1) is important. The inelastic processes are taken into account through the complex part of the optical potential via absorption potential. The complete spherical complex optical potential (SCOP) [18, 19] is represented by,

$$V_{opt}(E_i, r) = V_R(E_i, r) + iV_I(E_i, r) \quad (2)$$

where, the real part V_R consists of static potential (V_{st}), exchange potential (V_{ex}), and polarization potential (V_p). Owing to the fixed nuclei approximation, the static potential, (V_{st}) is calculated at the Hartree-Fock level. The exchange potential (V_{ex}) is responsible for electron exchange between the incoming projectile and one of the target-electrons. The polarization potential (V_p) combines the short range correlation and long range polarization effect that arises due to the momentarily redistribution of target charge cloud which gives rise to dipole and quadrupole moments. The second term of equation (2), V_I , is the imaginary part of the potential which is taken care by

*Corresponding author: barotavani29@yahoo.com

absorption potential. It is to be noted here that the spherical complex optical potential (SCOP) as such does not require any fitting parameters. All the potentials described vide equation (2) are charge-density dependent. Hence, representation of target charge density is very crucial. We have employed atomic charge density derived from the HartreeFock wave functions of Salvat et al [20]. In the SCOP formalism, the spherical part of the complex optical potential is used to solve exactly the Schrödinger equation using partial wave analysis to yield various cross sections. Presently our absorption potential is elastic to both vibrational and rotational excitations of the target.

As discussed earlier the absorption potential takes care of loss of flux into all allowed inelastic channels. For this we have used model potential of Staszewska et al [21] which is non-empirical, quasifree, Pauli-blocking and dynamic in nature. The full form of model potential is represented by,

$$V_{abs}(r, E_i) = -\rho(r) \sqrt{\frac{T_{loc}}{2}} \times \left(\frac{8\pi}{10 k_F^3} \right) \times \theta(p^2 - k_f^2 - 2\Delta) \cdot (A_1 + A_2 + A_3) \quad (3)$$

The parameters A_1 , A_2 and A_3 are defined as,

$$A_1 = 5 \frac{k_f^3}{2\Delta}; \quad A_2 = \frac{k_f^3 (53p^2 - k_f^2)}{(p^2 - k_f^2)^2};$$

$$A_3 = \frac{2\theta(2k_f^2 + 2\Delta - p^2)(2k_f^2 + 2\Delta - p^2)^{5/2}}{(p^2 - k_f^2)^2}. \quad (4)$$

The local kinetic energy of the incident electron is given by,

$$T_{loc} = E_i - (V_{st} + V_{ex}) \quad (5)$$

The absorption potential is a function of atomic/molecular charge density ($\rho(r)$), incident energy (E_i) and the parameter Δ of the target. It is not sensitive to long range potentials like V_{pot} and hence is neglected in local kinetic energy term of equation (3). In equation (2), $p^2 = 2E_p$ is the energy of incident electron in Hartree, $k_f = [3\pi^2 \rho(r)]^{1/3}$ is the Fermi wave vector. Further $\theta(x)$ is the Heaviside unit step-function, such that $\theta(x) = 1$ for $x \geq 0$, and is zero otherwise. The dynamic functions A_1 , A_2 and A_3 of equation (2) depend differently on $\rho(r)$, I (ionization potential of the target), Δ and E_i . The parameter Δ determines a threshold below which $V_{abs} = 0$, and the ionization or excitation is prevented energetically. This means the Δ parameter represents the threshold energy for continuum states: only ionization processes are taken into account, excitation to discrete levels being ignored by the original model [22]. So in order to include the excitations due to discrete levels at lower energy, we have considered Δ as a variable accounts for more penetration of the absorption potential in the target charge-cloud region [23-25]. Following the earlier works in this regard [23-25], we express

$$\Delta(E_i) = 0.8I + \beta(E_i - I) \quad (6)$$

Here, β is obtained by requiring that $\Delta = I$ at $E_i = E_p$ (Peak energy), where E_p is the value of E_i at which Q_{inel} attains maximum value. For $E_i > E_p$, Δ is held constant equal to Ionization energy of the target as suggested in the original model of Staszewska et al [21].

After generating the full complex optical potential given in equation (2) for a given electron molecule system, we solve the Schrödinger equation numerically with the 'Numerov method' using partial wave analysis. At low incident electron energies with short range potentials, only few partial waves are significant for convergence, e.g. at ionization threshold of the target around 5-6 partial waves are sufficient but as the incident energy increases large number of partial waves are needed for convergence. Using these partial waves the complex phase shifts are obtained which are key ingredients to find the relevant cross sections. The phase shifts contains all the information regarding the scattering event.

Total inelastic cross section determined vide equation (1) is not a directly measurable quantity and hence also not directly comparable quantity. However, experimentally the total inelastic cross sections can be obtained as the difference between experimental values of grand total cross sections (beam attenuation experiments) and purely elastic cross sections (obtained by integrating the differential elastic cross sections). In practice few experimental groups are doing both the measurements simultaneously, and different groups work in different energy regimes and their experimental uncertainties are also different and hence there is difficulty in obtaining total inelastic cross sections from the experiment. But, it is one of the most important quantities as it contains the ionization and electronic excitations which are directly measurable quantities. Thus, we partition the total inelastic cross sections into its two vital components one due to the discrete electronic excitations and other due to the continuum ionization contribution, as

$$Q_{inel}(E_i) = \sum Q_{exc}(E_i) + Q_{ion}(E_i) \quad (7)$$

Here, first term represents the sum over total excitation cross sections for all accessible electronic discrete transitions, while the second term is the total cross section due to all allowed electronic transitions to continuum i.e. ionization. In the present range of energies it is the single ionization that dominates in equation (7). The discrete transitions arise mainly from the low-lying dipole allowed transitions for which the cross section decreases beyond E_p . By definition,

$$Q_{inel}(E_i) \geq Q_{ion}(E_i) \quad (8)$$

This is an important inequality and it forms the basis for CSP-ic method. The detailed discussion for CSP-ic could be found in earlier publications [25,26] and here only important details required for the present study is discussed.

Total ionization cross section may be estimated from total inelastic cross section by defining an energy dependent ratio $R(E_i)$ given by,

$$R(E_i) = \frac{Q_{ion}(E_i)}{Q_{nd}(E_i)} \quad (9)$$

such that, $0 < R < 1$.

As total ionization cross section is a continuous function of energy, we can express this ratio also as a continuous function of energy for $E_i > I$, used in earlier studies

$$R(E_i) = 1 - f(U) = 1 - C_1 \left(\frac{C_2}{U+a} + \frac{\ln(U)}{U} \right) \quad (10)$$

here, U is the dimensionless variable defined by, $U = \frac{E_i}{I}$

The reason for adopting such explicit form of $f(U)$ could be visualized as follows. At high energies the total inelastic cross section follows the Born Bethe term according to which the cross sections falls of as $(\ln(U)/U)$, but at low and intermediate energies they obey $(1/E)$ form [28]. Accordingly the first term will take care of the cross section behavior at low and intermediate energies while the second term will take care at high energy. The dimensionless parameters C_1 , C_2 and 'a' involved in the above equation are deduced by imposing the three conditions on the ratio as discussed below.

$$R(E_i) \begin{cases} = 0 & \text{for } E_i \leq I \\ = R_p & \text{for } E_i = E_p \\ \cong 1 & \text{for } E_i \gg E_p \end{cases} \quad (11)$$

The first condition is an exact condition wherein it states that no ionization process is possible below the ionization threshold of the target implying that the value of the ratio must be zero. Coming to the last condition, which physically states that ionization contribution is almost equal to inelastic contribution at very high ($\sim 10 E_p$) energies, this is attributed to the fact that at such high energies there are innumerable channels open for the ionization as against very few finite channels for electronic excitation. At such high energies the contribution of excitation is almost negligible. Thus the ratio approaches to unity.

The second condition is very crucial and is empirical in nature in CSP-ic method. R_p is the value of R at $E_i = E_p$, and it was observed that at the peak of inelastic cross section the contribution for ionization is about 70 to 80 % [25-29]. This argument was supported by many targets studied through CSP-ic. The results obtained using CSP-ic formalism is reported in the next section.

RESULTS AND DISCUSSION

The theoretical approach of SCOP along with the present CSP-ic method outlined above is employed to determine total inelastic cross sections, Q_{inel} and total ionization cross sections, Q_{ion} along with a useful byproduct of electronic excitations in terms of the summed cross section $\sum Q_{exc}$. In the present paper, we have investigated three atoms (Ba, Pb and U) of applied interest and computed the total ionization cross sections.

The ionization cross sections are plotted as function of projectile energy for Ba, Pb and U from threshold of the target to 2 keV vide Figures 1-3 respectively. The ionization threshold, the parameters ' C_1 ', ' C_2 ' and 'a' of the target along with peak energy of the ionization cross section is tabulated in Table 1 and the numerical values of the total ionization cross section are tabulated in Table 2 for ready reference.

Table 1: Complex Spherical Potential-ionization contribution (CSP-ic) parameters for Ba, Pb and U atoms.

Atom	Ionization threshold (eV)	Ionization Peak (eV)	Cross section at the peak (\AA^2)	C_1	C_2	a
Ba	5.21	15	15.54	-1.757	-5.293	8.302
Pb	7.42	30	7.66	-1.845	-5.365	8.900
U	6.19	25	9.76	-1.458	-8.542	11.452

Table 2: Total ionization cross sections, Q_{ion} (\AA^2) for U, Pb and Ba. Maximum values of the cross section are shown in the bold print.

Energy (eV)	Q_{ion} (\AA^2)	Q_{ion} (\AA^2)	Q_{ion} (\AA^2)	Energy (eV)	Q_{ion} (\AA^2)	Q_{ion} (\AA^2)	Q_{ion} (\AA^2)
	Ba	Pb	U		Ba	Pb	U
6	1.98	-----	0.00	90	8.58	5.32	7.13
7	5.13	0.00	0.76	100	8.02	5.74	6.89
8	8.07	0.30	2.39	150	6.20	4.96	5.89
9	10.45	1.11	3.89	200	5.14	4.32	5.18
10	12.25	2.00	5.25	250	4.50	3.80	4.58
12	14.42	3.70	7.30	300	3.84	3.41	4.09
15	15.49	5.57	8.98	350	3.26	3.06	4.73
17	15.54	6.36	9.49	400	2.87	2.80	3.32
20	15.31	7.05	9.73	500	2.24	2.35	2.73
25	14.54	7.52	9.76	600	1.87	2.03	2.34
30	13.87	7.66	9.50	700	1.50	1.82	2.07
40	12.77	7.37	8.96	800	1.34	1.62	1.80
50	11.61	7.03	8.54	900	1.24	1.45	1.63
60	10.98	6.68	8.19	1000	1.14	1.31	1.45
70	9.82	6.41	7.79	1500	0.89	0.92	0.96
80	9.18	6.14	7.44	2000	0.67	0.66	0.76

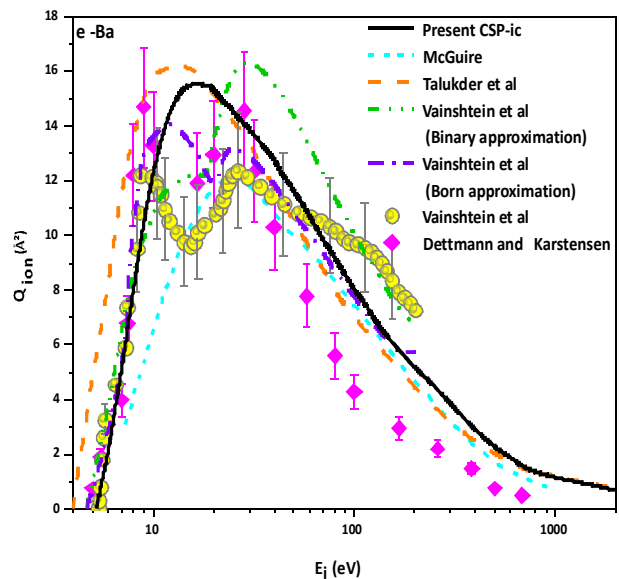


Fig. 1 (color online) Total ionization cross sections for e -Ba atom. Solid line, Present results; Solid Diamonds, Dettmann and Karstensen [3] Short Dash line, McGuire [4] and Dashed line, Talukder et al [5]; Dash dot line, Vainshtein et al (Born approximation)[6], Dash dot dot line, Vainshtein et al (Binary approximation)[6], Sphere with circle, Vainshtein et al [6].

Figure 1 shows comparison of e -Ba scattering with available data [3-6]. It is to be noted here that Ba cannot be found in pure state due to its readiness to form oxides, hence experiments are difficult. The measured total ionization cross sections are reported by Dettmann and Karstensen [3] and Vainshtein et al [6]. There are some structures observed in both measured data around 15 eV which are reproduced in theory given by Vainshtein et al [6] reported here. They have employed two different formalism Born approximation [7] and Binary approximation [8].

Present results are in very good agreement with both the measured values [3, 6] up to 12 eV. Afterward some disagreements are found up to 25 eV between measured data and our calculated data. After 25 eV to 30 eV some agreement with experiments available but above this energy, both the experimental data are separated and our calculated results lies in between their given data [3, 6]. Theoretical results are predicted by McGuire [4] and Talukder et al [5] and Vainshtein et al [6] in which they used two different formalisms (Binary approximation and Born approximation). Our results are in good agreement with the results of Vainshtein et al [6] (Born approximation) except the peak region. At a peak, some structure is observed in both methods of Vainshtein et al [6]. Recently Talukder et al [5] have predicted electron impact total ionization cross section for atoms with Z (1-92). The results of Talukder et al [5] are higher compared to all other data presented here and a leftward shift in the peak is observed. At high energy after 100 eV, all theories are found in agreement with each other. But the difference at the peak is observed in all the available results [3-6].

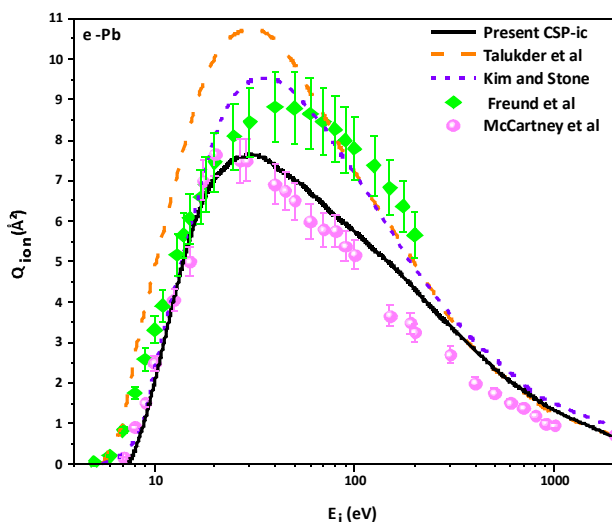


Fig. 2 (color online) Total ionization cross sections for e -Pb atom. Solid line, Present results; Dashed line, Talukder et al [5]; Diamonds, Freund et al [9]; Open Spheres, McCartney et al [10] and Short Dash line, Kim and Stone [11].

Figure 2 shows comparison of present data for e -Pb scattering with available data [5, 9-11]. There are two measurements reported by Freund et al [9] and McCartney et al [10]. Present data is in agreement with both the experiments up to 30 eV. After this energy, large difference observed between two experiments [9, 10] and our calculated data is in the agreement with McCartney et al [10] up to 100 eV. Above this energy the results reported by McCartney et al [10] underestimates to the all available data [5, 9, 11]. Our results are lying between both the experimental results up to 200 eV. There are also two theoretical predictions of Kim and Stone [11] and Talukder et al [5] available. The energy at the peak of the all theories is in agreement but large difference in cross sections observed between all of them the results of Kim and Stone [11] is 27% higher than our results and the data Talukder et al [5] about 50% higher than our calculated. But at high energies both the theories are in good agreement with the present data.

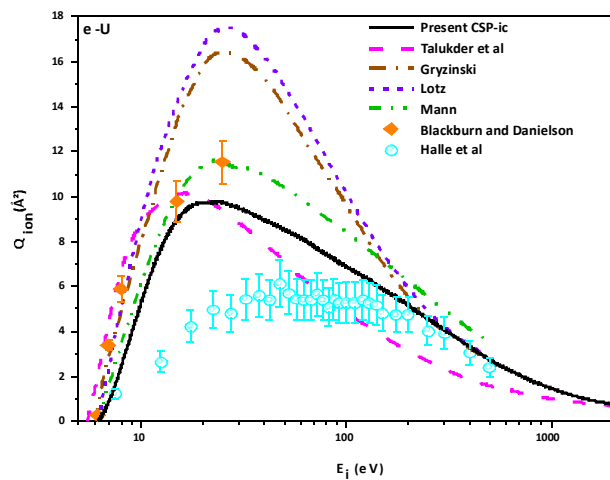


Fig. 3 (color online) Total ionization cross sections for e -U atom. Solid line, Present results; Dashed line, Talukder et al [5]; Open Spheres, Halle et al [13]; Open stars, Blackburn and Danielson [14]; Dash-Dot-Dot line, Mann [15]; Dash-Dot line, Gryziński [16]; and Short Dash line, Lotz [17].

Finally in Figure 3 we compare present data for e -U scattering with data in the literature [5,13-17]. There are more theoretical investigations [5,15-17] compared to measurements [13,14]. The measurements are provided by Halle et al [13] and Blackburn and Danielson [14]. Both the measurements [13,14] show vast variation in their nature. Present results are lying between both the experiments. After 100 eV, our data are lying in the error bar region of the experimental results of Halle et al [13] and after 200 eV it merges with the experimental as well as other theoretical data [13, 16, 17]. At low energy region up to 15 eV, our data are in good agreement with the given theoretical data by Mann [15]. Except Talukder et al [5], the peak energy of all other theories are in agreement around 25 eV. The problem found with the cross section values at the peak energy. The cross section value at the peak energy for the present result is 9.76 \AA^2 . At the peak energy, the present cross section is approximately half compared to the calculated data by Lots [17]. The cross section of Talukder et al [5] is around 5% higher; Mann [15] is 11% higher and Gryziński [16] is 65% higher than present result of cross section at peak. But the peak value of experimental data provided by Halle et al [13] is around 6.13 \AA^2 which is found to be very low compared to all

theories and the present cross section seems lower compared to other available data. For U also as observed in case of Ba and Pb the peak is shifted and value is slightly higher at the peak as Talukder et al [5].

CONCLUSION

A series of calculations to obtain total ionization cross sections for Ba, Pb and U atoms were carried out. We have employed the well-known SCOP and CSP-ic formalisms to perform these calculations. It is to be noted here that lower ionization threshold results in to lower peak energy and higher cross sections. This is very clearly evident from Table 1. Considering present targets, Ba has lowest ionization threshold (5.21 eV) so lower peak energy (15 eV) and maximum cross section (15.54 \AA^2), U has 6.29 eV ionization threshold, 25 eV peak energy and 9.76 \AA^2 cross section and finally Pb has highest ionization threshold (7.42 eV) and hence higher peak energy (30 eV) and lowest peak cross sections (7.66 \AA^2). The total ionization results obtained are presented in the article numerically in Table 2 and are compared with other available measurements and theories vide graphs 1-3. Large discrepancies in measurement and theory make this study very imperative, since most of the previous studies are fragmented. The present method calculates the total ionization resulting from single, double or higher order partial ionization cross sections. But it is not possible to distinguish the fraction of contribution from different channels nor it is possible to calculate the ionization cross section orbital shell or subshell. Hence it is not able to distinguish the giant resonances resulting from 4d electrons [30]. This is the limitation of this method. We find that the present results are over all consistent in strength and shape and hence prove that present method can produce reliable cross sections. So it can be easily employed for the targets where experiments are difficult.

ACKNOWLEDGEMENT

MVK is thankful to DST, New Delhi, for Major Research Project under which part of this work is carried out.

REFERENCES

- [1] Smith P. T. (1930), The Ionization of Helium, Neon, and Argon by Electron Impact, *Phys. Rev.*, **36**: 1293.
- [2] Compton K. T. and Langmuir I. (1930), Electrical Discharges in Gases. Part I. Survey of Fundamental Processes, *Rev. Mod. Phys.*, **2**: 123.
- [3] Dettmann J.-M. and Karstensen F. (1982), Absolute ionisation functions for electron impact with barium, *J. Phys. B: At. Mol. Phys.*, **15**: 287.
- [4] McGuire E. J. (1979), Scaled electron ionization cross sections in the Born approximation for atoms with $55 \leq Z \leq 102$, *Phys. Rev. A*, **20**: 445.
- [5] Talukder M. R., Bose S., Patoary M. A. R., Haque A. K. F., Uddin M. A., Basak A. K. and Kando, M. (2008), Empirical model for electron impact ionization cross sections of neutral atoms, *Eur. Phys. J. D.*, **46**: 281.
- [6] Vainshtein L.A., Ochkur V.I., Rakhovskrl V.I., and Stepanov A.M. (1972), Absolute values of electron impact ionization cross sections for Magnesium, Calcium, Strontium and Barium, *Soviet Physics JETP*, **34**: 271
- [7] Beigman I. L. and L.A. Vailnshtein, *Astr. Zh.* **44**, 887 (1967) [*L. Sov. Astron.-AJ* 11, 712 (1968)]
- [8] Stabler R. (1964), Classical Impulse Approximation for Inelastic Electron-Atom Collisions, *Phys. Rev.* **133**, A1268
- [9] Freund R. S., Wetzel R. C., Shul R. J. and Hayes T. R. (1990), Cross-section measurements for electron-impact ionization of atoms., *Phys. Rev. A*, **41**: 3559.
- [10] McCartney P. C. E., Shah M. B., Geddes J. and Gilbody H. B. (1998), Multiple ionization of lead by electron impact, *J. Phys. B: At. Mol. Opt. Phys.*, **31**: 4821.
- [11] Kim Y.-K. and Stone P. M. (2007), Ionization of silicon, germanium, tin and lead by electron impact, *J. Phys. B: At. Mol. Opt. Phys.*, **40**: 1597.
- [12] Blaise J. and Radziemski L. J. (1976), Energy levels of neutral atomic uranium (U I), *Jr., J. Opt. Soc. Am.*, **66**: 644.
- [13] Halle J. C., Lo H. H. and Fite W. L. (1981), Ionization of uranium atoms by electron impact, *Phys. Rev. A*, **23**: 1708.
- [14] Blackburn P. E. and Danielson P. M. (1972), Electron Impact Relative Ionization Cross Sections and Fragmentation of U, UO, UO₂, and UO₃, *J. Chem. Phys.*, **56**: 6156.
- [15] Mann J. B. (1967), Ionization Cross Sections of the Elements Calculated from Mean-Square Radii of Atomic Orbitals, *J. Chem. Phys.*, **46**: 1646.
- [16] Gryziński M. (1965), Classical Theory of Atomic Collisions. I. Theory of Inelastic Collisions, *Phys. Rev.*, **138A**: A366.
- [17] Lotz W. (1967), Electron-impact ionization cross-sections and ionization rate coefficients for atoms and ions, *Astrophys. J. Suppl. Ser.*, **14**: 207.
- [18] Jain A. and Baluja K. L. (1992), Total (elastic plus inelastic) cross sections for electron scattering from diatomic and polyatomic molecules at 10-5000 eV: H₂, Li₂, HF, CH₄, N₂, CO, C₂H₂, HCN, O₂, HCl, H₂S, PH₃, SiH₄, and CO₂, *Phys. Rev. A*, **45**: 202.
- [19] Jain A. (1986), Total (elastic+absorption) cross sections for e-CH₄ collisions in a spherical model at 0.10-500 eV, *Phys. Rev. A*, **34**: 3707.
- [20] Salvat F., Martinez J. D., Mayol R. and Parellada, J. (1987), Analytical Dirac-Hartree-Fock-Slater screening function for atoms (Z = 1 - 92), *Phys. Rev. A*, **36**: 467.
- [21] Staszewska G., Schwenke D. W., Thirumalai D. and Truhlar D. G. (1983), Quasifree - scattering model for the imaginary part of the optical potential for electron scattering, *Phys. Rev. A*, **28**: 2740.
- [22] Blanco F. and Garcia G. (2003), Improvements on the quasifree absorption model for electron scattering, *Phys. Rev. A*, **67**: 022701.
- [23] Vinodkumar M., Korot K. and Vinodkumar P. C. (2010), Complex scattering potential - ionization contribution (CSP-ic) method for calculating total ionization cross sections on electron impact, *Euro. Phys. J. D.*, **59**: 379.
- [24] Joshipura K. N., Vinodkumar M., Limbachiya C. G. and Antony B. K. (2004), Calculated total cross sections of electron-impact ionization and excitations in tetrahedral XY₄ and SF₆ molecules, *Phys. Rev. A*, **69**: 022705.

- [25] Joshipura K. N., Antony B. K. and Vinodkumar M. (2002), Electron scattering and ionization of ozone, O₂ and O₃, *J. Phys. B: At. Mol. Opt. Phys.*, **35**: 4211.
- [26] Vinodkumar M., Joshipura K. N., Limbachiya C. G. and Antony B. K. (2009), Atomic Structure and Collision Processes, *Narosa Publishing House*, p.177.
- [27] Vinodkumar M., Limbachiya C. and Bhutadia H. (2010), Electron impact calculations of total ionization cross sections for environmentally sensitive diatomic and triatomic molecules from threshold to 5 keV, *J. Phys. B: At. Mol. Opt. Phys.*, **43**: 015203.
- [28] Joshipura K. N., Vinodkumar M., Antony B. K. and Mason N. J. (2003), Theoretical total ionization cross-sections of CH_x, CF_x, SiH_x, SiF_x (x = 1–4) and CCl₄ targets by electron impact, *Euro. Phys. J. D.*, **23**: 81.
- [29] Vinodkumar M., Limbachiya C., Antony B. and Joshipura K. N. (2007), Calculations of elastic, ionization and total cross sections for inert gases upon electron impact: threshold to 2 keV, *J. Phys. B: At. Mol. Opt. Phys.*, **40**: 3259.
- [30] Younger, S. M; (1987) Systematics of giant resonances in the electron-impact ionization of heavy atoms and ions: Ionization of the 4d subshell, *Phys. Rev. A*, **35**: 4567